

Image Monitoring Study on Fused Deposition Modeling (FDM) Fabrication Process

Hung-Yin Tsai*, Wei-Yuan Hsu**, Yi-Hung Chen*** and Che-Chih Tsao****

Keywords: Additive Manufacturing, Fused Deposition Modeling(FDM), Image Monitoring

ABSTRACT

Fused Deposition Modeling (FDM), a convenient method to manufacture complex parts, has its drawbacks of uncontrollable defects, which often results in low precision of the desired product. An image-based monitoring system for plastic material FDM technology has been proposed in this study. During the FDM process, images of the nozzle are captured through the monitoring system. By calculating the real-time height, width and gathering pixel information of the product profile, criterions are then established to control the feed of the nozzle which can, in turn, ameliorate the precision and quality of the product.

1. INTRODUCTION

Compared to conventional subtractive machining methods, such as CNC milling, additive manufacturing can produce more delicate structures. However, most of the existing FDM techniques lacks real-time feedback mechanisms that allow the system to monitor the quality of the workpiece while fabricating.

Traditionally, the quality control in manufacturing industry was done manually. Since the 1980s, some researchers have proposed algorithms of surface-defect detection for different types of materials, for example, food, textiles, etc. (Zhang et al., 2014) (Ngan et al., 2011). Image processing is an innovative method used in the production line of the manufacturing industry, which saves labor costs, increases the efficiency of defect detection, and ensures the quality of the workpiece.

Paper Received July, 2018. Revised October, 2018. Accepted November, 2018. Author for Correspondence: Hung-Yin Tsai

** Professor, Department of Power Mechanical Engineering, National Tsing Hua University, Hsinchu, Taiwan, ROC*

*** Master, Department of Power Mechanical Engineering, National Tsing Hua University, Hsinchu, Taiwan, ROC*

**** Ph.D. student, Department of Power Mechanical Engineering, National Tsing Hua University, Hsinchu, Taiwan, ROC*

***** Assistant Professor, Department of Power Mechanical Engineering, National Tsing Hua University, Hsinchu, Taiwan, ROC*

An image-based FDM process monitoring method is proposed in this study. The goal is to improve the precision of the new homemade FDM machine.

2. LITERATURE REVIEW

2.1 Introduction of FDM

FDM, a branch of the additive manufacturing technology, is a machining technique developed by the American Crump in the 1980s that was patented in 1989 (Crump et al., 1996). To produce a workpiece, 3D CAD models could be produced by a computer aided design (CAD), then transformed into an STL file (Pamdey et al., 2003). The STL file contains the G code which has the information of the moving path of the extrusion head. After loading the STL file, the machine will then move accordingly, printing the desired three-dimensional object layer by layer.

2.2 Defects of FDM

During the process of FDM, if the parameters are non-ideal, defects would be present on the workpiece. Agarwala et al. (1996) mentioned two main defect types of the FDM technique – surface defects and internal defects. These two types of defects alongside with three-dimensional defects are discussed in the following sections.

2.2.1 Surface Defects-Defects on the origin and destination of the contour

As shown in Fig. 1 (Agarwala et al., 1996), these lines are the path of extrusion nozzle. The circle at the outside is contour and the lines other than the contour is the raster.

When the contour is almost complete, the traveling speed of extrusion nozzle could not match the speed of filament feeding motor, therefore a visible protrusion at the junction of the origin and destination was formed, as shown in Fig. 2 (Agarwala et al., 1996).

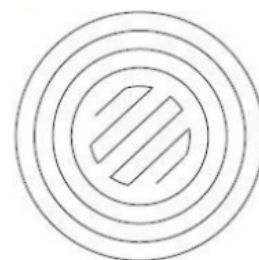


Fig. 1 Path planning pattern. (Agarwala et al., 1996)

2.2.2 Internal defects

The followings are some common types of internal defects:

(1) Non-sequential raster segments

As shown in Fig. 3 (Boschetto et al., 2016), the raster of this CAD file is separated into two or more paths. This implies different cooling regions, i.e., one region cools down and solidifies before the other, which means that the bonding strength of the plastic between regions will be not as strong as the bonding strength of the plastic in the same region.

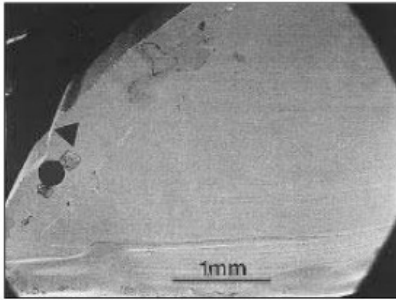


Fig. 2 ●: The origin of the contour ▲: The destination of the contour. (Agarwala et al., 1996)

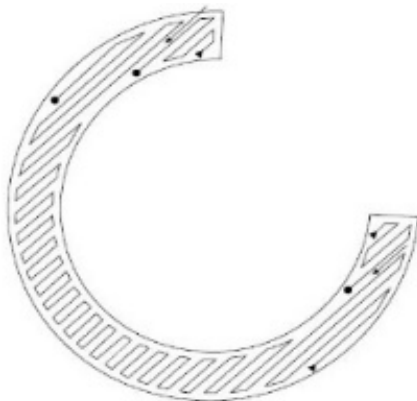


Fig. 3 ▲: Starting point ●: Ending point (Boschetto et al., 2016)

(2) Inter-road defects

Between two adjacent extrusion paths, there exist two types of defects. Firstly, the voids between adjacent extruded materials, as shown in Fig. 4 (Boschetto et al., 2016). Secondly, an inter-road void that is seen in a single extrusion path, as shown in Fig. 5 (Wu et al., 2003). Both conditions affects the strength of the resulting structure severely.

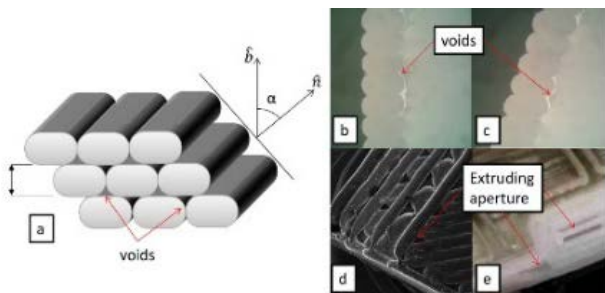


Fig. 4 Voids (Boschetto et al., 2016).

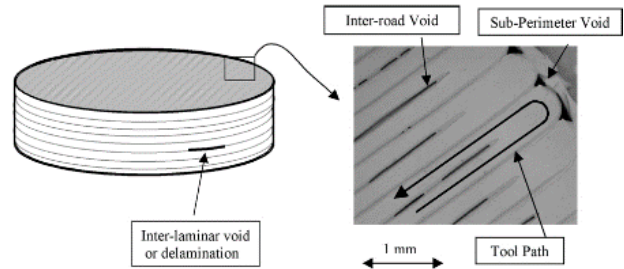


Fig. 5 Inter-road void (Wu et al., 2003).

(3) Non-uniform filament diameter

Under the condition that all parameters, such as feed rate, are fixed and normal, if the diameter of the filament is non-uniform, it is highly possible to result in the non-uniform diameter of the extruded materials.

2.2.3 Three-dimensional defect

So far, studies that discuss defects of additive manufacturing are mainly focused on two-dimensional defects; three-dimensional defects are yet to be explored. Hence, methods of detecting three-dimensional defects are referenced from other research fields.

Bhandarkar et al. (2006) used computed tomography (CT) to detect the position and type of defect inside wood. The research method of Bhandarkar et al. provides great insight and a feasible solution for future work of this study.

2.3 Defect detection method of FDM

During the FDM process, different types of defects, discussed in section 2.2, might occur. Detection of the formation of defects in real-time is considered as an important issue. The followings summarize methods of defect detection that were proposed in recent studies.

2.3.1 Signature analysis Method

Fang et al. (2003) defined signature as the gray scale value distribution along the path of extrusion. The signature data was obtained and stored into a feature vector. In that study, they printed a sensor and actuator using ceramic by the home-made FDM machine. First, the planned path of the extrusion head generated by decoding the CAD file. As shown in Fig. 6 (Fang et al., 2003), the superimposed image is then dissected into two parts – the contour and the raster.

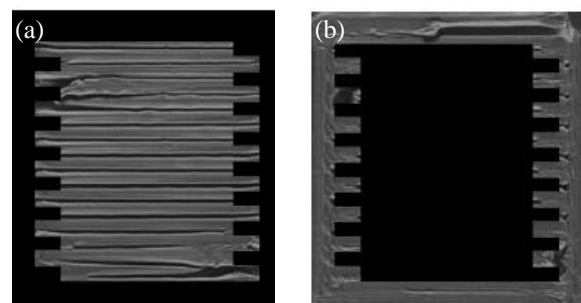


Fig. 6 The pattern of contour and raster. (a) Contour; (b) Raster (Luo et al., 2001)

Next, using the detection algorithm, signatures were recognized. By synthesizing the selected signatures, ideal

contour and raster images are formed, as shown in Fig. 7 (Fang et al., 2003).

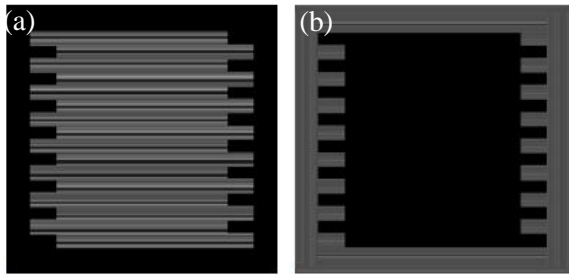


Fig. 7 Ideal contour and raster pattern. (a) Contour; (b) Raster (Fang et al., 2003)

Finally, by comparing the original and ideal images, underfilled and overfilled regions can be detected, as shown in the gray areas in Fig. 8 (Fang et al., 2003).



Fig. 8 Defect image (Fang et al., 2003)

2.3.2 Correlation method

Luo et al. (2001) compared the ideal image (photomask image) and the actual image after one layer of deposition. After analyzing the difference between the two images, he proposed a correlation formula that can calculate the relation between the ideal and captured images:

$$r = \frac{N \sum IM - \sum I \sum M}{\sqrt{[N \sum I^2 - (\sum I)^2] [N \sum M^2 - (\sum M)^2]}} \quad (1)$$

In the above formula, I is the adjacent pixels, M is the pixels of the comparison image, and N represents the pixels of the ideal image.

After calculating the correlation value r between the actual and ideal images, a second formula called the match score formula was proposed:

$$\text{Match Score} = \max(r, 0)^2 \times 100 \quad (2)$$

where r is the correlation value, calculated in equation (1).

Due to the unpredictable nature of the additive manufacturing process, a perfect match score of 100 is nearly impossible to achieve, but satisfying values of 90 to 100 are expected. The relation between multiple images are listed in Table 1.

2.4 Clad Dimension Estimation of Metal Additive Manufacturing

Laser Cladding is a metal additive manufacturing technology which uses a laser as the heat source to deposit metal powder. As shown in Fig. 9 (Asselin et al., 2005), Asselin et al. (2005) proposed an image-based process monitoring system. During cladding process, there were three Charge-Coupled Device (CCD) cameras capturing images near the molten area. The images were then processed into black and white images.

Based on the direction of material deposition, the algorithm chooses images from two of the three CCD cameras. After transforming the pixel information of the images into the same coordinate system, the size of the molten area was then calculated. Once the clad dimension information was obtained, the algorithm checked whether dimension error is acceptable. This is a simple quality management method for the metal additive manufacturing process.

Table 1 Images after processed (Luo et al., 2001)

	Image of photomask	Image 1	Image 2
Actual image			
After processed			
Correlation		90%	76%

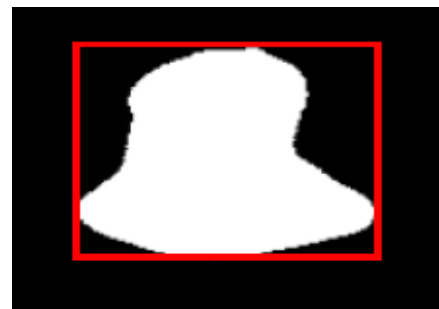


Fig. 9 Cladding area image (Asselin et al., 2005)

2.5 Image Segmentation

The thresholding method was proposed to separate a specific object from an image. As shown in Fig. 10, the ordinate of the diagram represents the number of points and the abscissa shows gray level value. It shows the distribution of the grayscale of the entire image. The optimal threshold value t is selected as a threshold value, to identify the object. However, the threshold value of the thresholding method is a fixed constant that cannot be adjusted in real-time. Therefore, Nobuyuki Otsu (1979) proposed an algorithm to select the threshold value according to the grayscale distribution of each image.

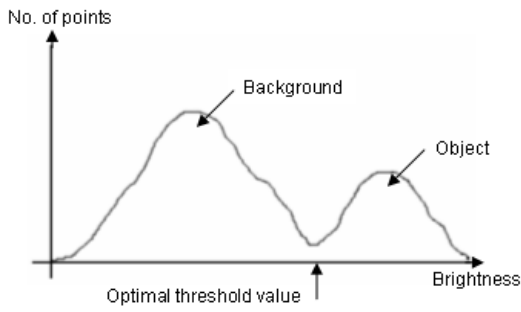


Fig. 10 Grey scale value distribution (Otsu, 1979)

3. RESEARCH METHOD

In section 2, the correlation between the quality of FDM objects and the characteristics of the extruded material were discovered. Even under optimal conditions where the nozzle head of the FDM machine follows the machine code, surface and internal defects might still occur, because of the non-uniform and uncontrollable nature of extruded material. The current FDM system is an open-loop system that lacks controlling mechanisms to monitor the process in real-time. In this study, we propose a controlling method to monitor the deposition modeling process. First, all parameters are initialized. Then, the images of the extrusion nozzle are loaded and the top surface and the side surface of extruded material are recognized. After that, a sampling point is set as a reference point to calculate the dimension of extruded material. The algorithm also confirms whether the printing process is finished and it will stop the detection once the printing process is completed. During the process, any abnormal aspect ratios will issue warnings to notify the user.

Each step of the proposed method is described in detail in each subsection below.

3.1 Nozzle Recognition

Images are captured by CCD cameras. The better the image quality and resolution, the more accurate the results of image processing.

Since the area around nozzle has the information of extruded parts right after deposition, it is of utmost importance and this study defines it as the region of interest (ROI). A flow chart in a literature written by Gauglitz et al. (2011) is cited to explain how the algorithm process and deciphers the ROI information, as shown in Fig. 11.

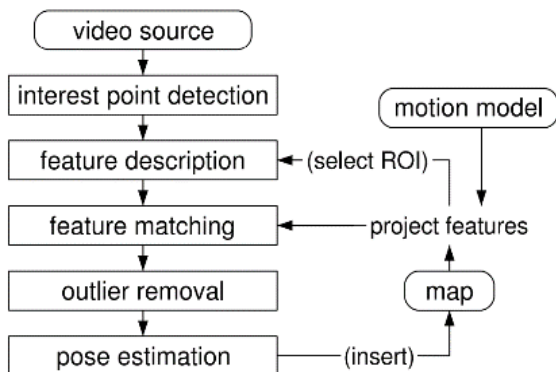


Fig. 11 ROP and ROI sampling flow chart (Gauglitz et al., 2011).

3.2 Top surface and side surface of extruded material Recognition

The cross section of the extruded material reassembles a rectangular shape right after it is extruded from the nozzle. The top surface and side surface of extruded material are defined, as shown in Figs. 12 and 13. Due to the planar light lighting in a specific angle near the nozzle, the reflection of light is different from each surface. Thus, surfaces are distinguished according to their respective gray scale values. The surface with higher average grayscale level value is defined as the top surface, while the surface with lower average gray scale value is defined as the side surface. The purpose of defining top and side surface is to calculate height and width information. The top surface is used to calculate the width, and the side surface is used to calculate the height.

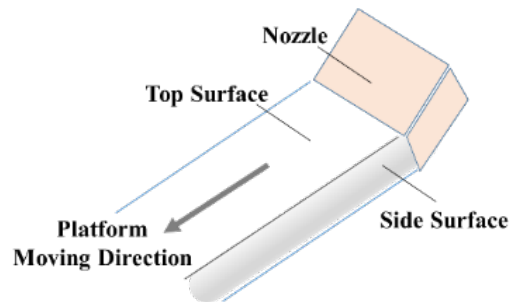


Fig. 12 Top surface and side surface of extruded material

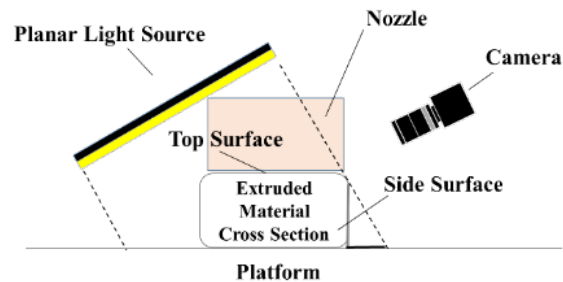


Fig. 13 Light source and camera set up

3.3 Dimension measurement

In section 3.1, after the nozzle was found in the image, a sampling point is set at a location near the nozzle, as shown in Fig. 14. The location of sampling point is at the ridge, where the top and side surfaces meet. The sampling point is a reference point that can be used to identify different surfaces. The red dotted line area is the area that is monitored, as shown in Fig. 14.

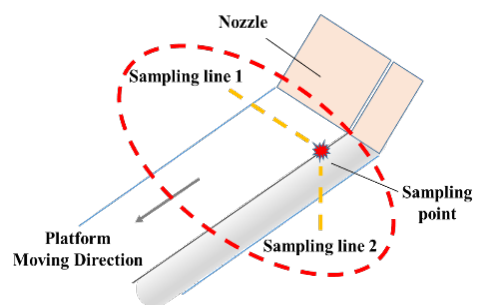


Fig. 14 Dimension measurement area

The edge of extruded material is detected by image binarization. Then, two sampling lines are defined. The direction of sampling line 1 is perpendicular to the direction of material extrusion and parallel to the nozzle outlet. The direction of sampling line 2 is vertical. Sampling line 1 is used to calculate the width information, while sampling line 2 is used to calculate the height information, as shown in Fig. 14.

The width information is obtained by counting the total number of pixels with a specific grayscale level (so that we only count pixels that are on the surface) value passing through sampling line 1. As shown in Fig. 15, sampling line 1 is a line parallel to the nozzle form P_1 to P_n , where P_n represents the sampling point.

The method of determination height is similar to the width's method, as shown in Fig. 16. Assuming that P_1 is a sampling point, the algorithm counts pixels with specific gray scale values along sampling line 2. In order to simplify the calculation, sampling line 2 extends along the X direction.

Then, the algorithm uses Otsu's method to separate the top surface and side surface and highlights pixels of different surfaces. The total number of pixels passing through sampling line 1 and line 2 are calculated respectively and the height and the width (in number of pixels) are obtained. This method successfully estimates the height and width of the extrusion.

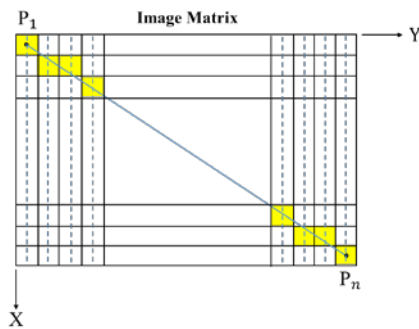


Fig. 15 Width calculation image matrix

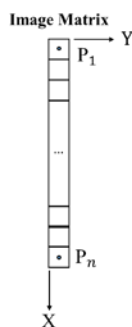


Fig. 16 Height calculation image matrix

3.4 FDM Quality Detection

The following differences between the actual experimental test platform and a conventional FDM machine are considered:

1. The width of extruded material is not fixed.
2. The extrusion path is three dimension.

In section 2.2, the method proposed was based on the

fact that the width of the FDM process is fixed. This method of determination of the quality of conventional FDM process cannot be implemented in this new type of FDM process. Therefore, this study proposes a method for determining the dimension of the extruded material and a criterion to monitor the quality of the extrusion in real time. This criterion checks that whether there is any sudden change in height and/or width, or whether the height and/or width are gradually increased or decreased in the long term.

The height and width information can be calculated by the software during the process of FDM in this study. The criteria used to achieve quality management is as follows: whenever the width of the extruded material exceed 20% or the height exceeds 40% of its stable size in this study, it is considered as an error situation. With the criterion, we could effectively monitor the deposition process.

4. EXPERIMENTAL RESULT AND DISCUSSION

4.1 Experimental setup

In this study, the new type FDM machine is homemade as shown in Fig. 17. It is a Shirline 8540 tabletop CNC milling machine platform with a new type of FDM system is fixed on it. The heater of the FDM machine is PACE ST25, and the extrusion material used is Polylactic Acid (PLA). PLA is extruded along the X axis direction on the platform.

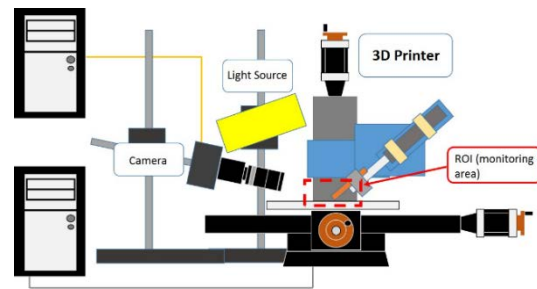


Fig. 17 Experimental setup

In Fig. 18, C_1 represents the location of CCD camera. O_1 is the exit of the nozzle. L_1 is the distance between exit and camera which is approximately 31.62 mm. θ_1 is approximately 34.7 degrees and the inclined angle θ_2 is approximately 22 degrees.

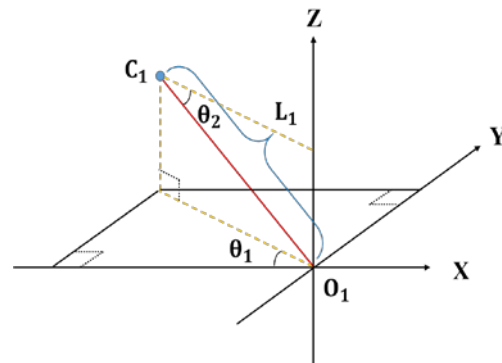


Fig. 18 Light source location parameters.

The location of the light source is shown in Fig. 19, where C_2 is the location of the light source. O_1 is the location

of the nozzle. L_2 is the distance between the light source and the exit of the nozzle which is approximately 9.988 mm. L_3 is the height of light source holder which is approximately 14 mm. L_4 is the distance of light source holder and the exit of the nozzle which is approximately 11.4 mm. θ_1 is approximately 50 degrees, θ_2 is approximately 34.7degrees, and θ_3 is approximately 29.44 degree. The light source lights up the extruded material from the top.

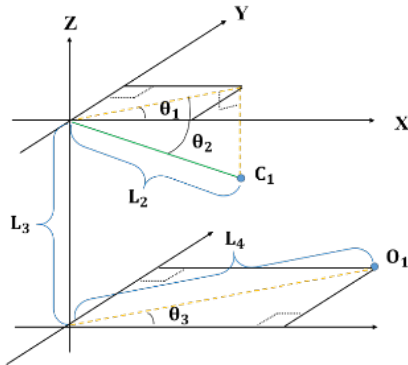


Fig. 19 Schematic of camera location parameters

Angular control is achieved by two Tower Pro MG995 servo motors. The moving speed of CNC platform is 50 mm/min. The temperature of the heater is 350°C. The inlet speed of filament is 6.1 mm/s. The fps of the camera is 60 and the image has a resolution of 1296 x 1032.

4.2 Image acquisition equipment

The CCD camera used in the current study is BFLY-PGE-14S2C-CS made by Point Grey. It has a resolution of 1296 x 1032, along with a maximum frame per second (fps) of 60. The model of the camera lens is Tokina TC1614-3MPG. The reason that this study chooses REVOX SLIM planar light source is because planar light can provide the most uniform lighting and creates a significant contrast between the top surface and side surface.

4.3 Quality detection Experiment

Using the traditional method of quality inspection is unsuitable for this study due to the volatile nature of the extruded material of new type FDM machine. Hence in section 3 of this study, a new method to determine the quality of extruded material is proposed. Unlike the traditional method of detecting surface or internal defects, this study focus on whether the dimensions of the extruded material meet the standards.

In this study, the quality detection experiment starts off from a simple extrusion of a straight path and obtaining dimensional information.

4.4 Experimental Result and Discussion

4.4.1 Image Segmentation

To calculate the width of extruded material, the extruded material has to be segmented from the background by the image segmentation method. If using the thresholding method mentioned, a threshold value must be chosen subjectively. On the other hand, Otsu’s method can obtain optimal threshold value based on statistical average and

standard deviation of the image. Compared to thresholding method, Otsu’s method is more feasible in this case. Fig. 20 shows the images before and after processing by Otsu’s method.

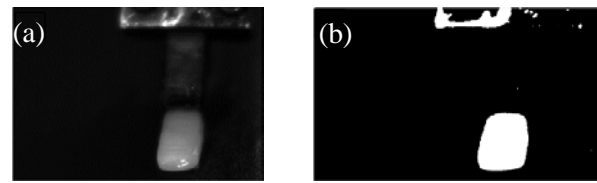


Fig. 20 Images before and after processing by Otsu’s method. (a) Original image; (b) Processed image.

4.4.2 Calculation of both height and width information

The 12 level Otsu’s method is chosen because it can obtain both height and width information simultaneously. Table 2 shows the gray scale value of the 12 levels within the image, where level 12 represents the brightest and level 1 represents the darkest pixels. The reason is that if fewer levels are chosen, the location of the ridge between the top and side surfaces will be ambiguous and the top surface and side surface pixels would be hard to distinguish.

Next, the height and width are calculated by the method mentioned in section 3.5. The brightest part of this image must be the top surface (level 12) while the background being the darkest one (level 1). The height of the extrusion possesses a mediocre brightness (level 2~level 11). The width information of extruded material is obtained by counting the total number of level 12 pixels that pass through the green line in Fig. 21 (a). Similarly, the height information is obtained by counting the total number of pixels passing through the blue line excluding the level 1 and level 12 pixels. Fig. 22 records the dimension information throughout the extrusion process.

Table 2 Threshold list.

Experiment Number \ Threshold level	1	2	3	4	5	Average
Level 1	15	17	16	16	18	16.4
Level 2	30	32	32	32	35	32.2
Level 3	51	53	53	53	56	53.2
Level 4	74	76	77	75	77	75.8
Level 5	101	100	101	97	97	99.2
Level 6	128	123	126	119	119	123
Level 7	149	140	146	142	140	143.4
Level 8	170	163	166	168	161	165.6
Level 9	190	186	189	187	182	186.8
Level 10	215	210	216	216	205	212.4
Level 11	240	235	238	236	229	235.6
Level 12	250	245	251	249	246	248.2
Gray scale value difference between Levels 12 and 11	10	10	13	13	17	12.6
Gray scale value percentage difference between Levels 12 and 11	3.92	3.92	5.098	5.098	6.667	4.9406

Fig. 21 (a) is an image processed by Otsu’s method after the level number is set to 12 where the original image is shown in Fig. 21 (b).

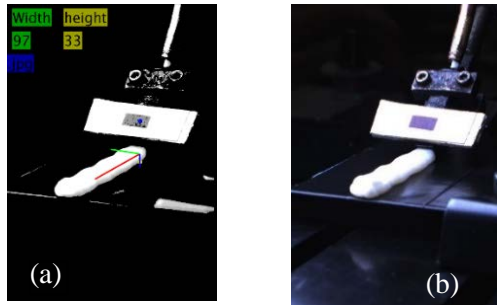


Fig. 21 Calculation of both height and width. (a) Processed image; (b) Original image.

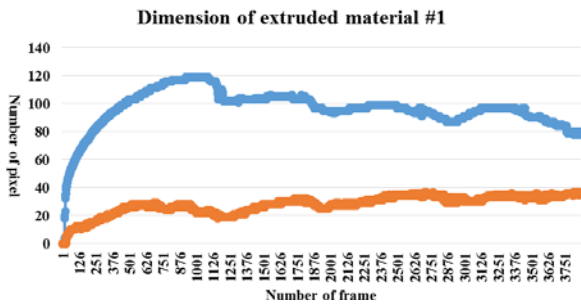


Fig. 22 Dimension information in every frame

4.5 Discussion

This goal of this study focuses on whether there is any error situation of dimension when the material is extruded so that quality of the extruded material can be effectively controlled. The following discussion is divided into two parts: the contrast of different surfaces under lighting is discussed; while in the second part, the demonstration how quality management can be achieved by setting up criterions.

4.5.1 Contrast of image

Table 2 shows five sets of experimental results under same experimental setup. Looking at experiment number 1, the gray scale value of the top surface, level 12, is 250 and the brightest gray scale value of the side surface, level 11, is 240.

It is evident that the minimum difference of the gray level value of the top surface and the brightest fraction of the side surface is 10. This represents a difference of 3.92 percentage among the grayscale value. In other words, the experimental setup should guarantee at least 4 percentage of image contrast every time so the top and side surface can be distinguished from each other. This is quite important since we need an accurate estimate of the current length of the top surface.

4.5.2 Quality quantization criteria

In order to evaluate the condition of the extruded material and obtained quality, a criterion is proposed to monitor the FDM process and evaluate the possibility of the product matching the desired parameters.

Under conditions of the experimental setup of section 4.1, the following parameters are used: Image capturing speed of the camera is 60 fps. Inlet speed of filament is 6

mm/s, moving speed of platform is approximately 1.667 mm/s, and the algorithm compares the dimension variation percentage of the present frame and the past 120 frames.

The dimension variance formula needs a correction term s that takes the speed of the platform into account. The dimension variance formula is as follows:

$$\text{Width Variance} = \left(\frac{\text{Width}(i) - \text{Width}(i - 60 \times \frac{1.667}{s})}{\text{Width}(i - 60 \times \frac{1.667}{s})} \right) \times 100\% \quad (3)$$

$$\text{Height Variance} = \left(\frac{\text{Height}(i) - \text{Height}(i - 60 \times \frac{1.667}{s})}{\text{Height}(i - 60 \times \frac{1.667}{s})} \right) \times 100\% \quad (4)$$

where 60 is the camera speed (fps), s is the moving speed of the platform (in mm/s)

If the inlet speed is greater than 6.1 mm/s, the aspect ratio of the extruded material becomes more stable. However, the ridge between the top and side surfaces of extruded material starts to become wavy because of the fast speed of the platform, as shown in Fig. 21.

As shown in Fig. 23 (ordinate represents the variance of dimension and abscissa represents the frame number), the greatest width variance is approximately 15 percent, and the greatest height variance is approximately 35 percent. The reason why the greatest percentage of the height variance is greater than the greatest percentage of the width variance is because the average number of height pixels is about 30 while the width is about 100. If both the height and the width increase or decrease by the same pixel number, the variance of the height would be greater.

After knowing the reasonable variance levels of the height and width, criteria can be established to monitor the extruded material in real time. This criterion is as follows: the height variance less than 40 percent and the width variance less than 20 percent. In order to avoid long-term trends of continual increasing or decreasing of height or width, the algorithm also checks the variance of dimension information between the current frame and the 500th frame prior to the present.

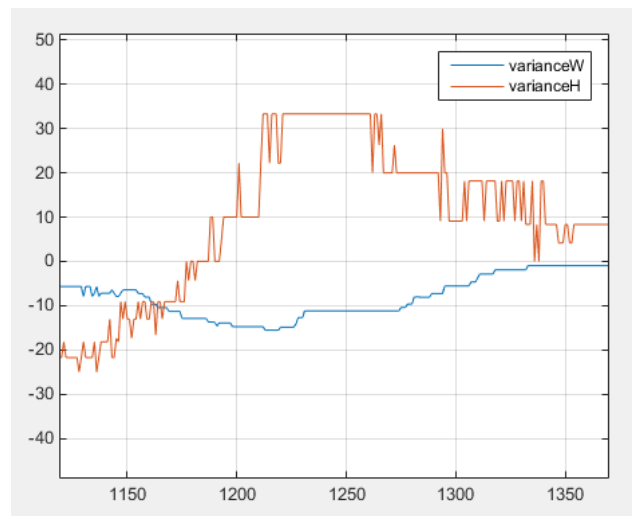


Fig. 23 Variance percentage of dimension

Currently, the new FDM is still unstable and cannot maintain the dimensions of the extruded material with

precision. This method can detect sudden and long term changes of the dimensions of the extruded material which is ideal to implement into controlling mechanisms of the machine in the future.

5. CONCLUSION

In the past, there is no suitable feedback system for FDM system to ensure the quality of the product. Quality can only be checked after the product is finished. If the quality of the product is unacceptable, there is no other way to adjust or remodel.

The main purpose of this study is to establish a quality monitoring method for the new type FDM system. In this study, the dimension information of the region of interest is calculated from consecutive images captured by a CCD camera. The proposed algorithm is used to check whether quality is acceptable by a criterion. This is an essential way of achieving quality management.

ACKNOWLEDGEMENTS

The authors greatly appreciate the support received from the National Ministry of Science and Technology of Taiwan under the contract number of MOST-105-2218-E-007-004.

REFERENCES

- Zhang, B., Huang, W., Li, J., Zhao, C., Fan, S., Wu, J. and Liu, C., "Principles, developments and applications of computer vision for external quality inspection of fruits and vegetables: A review." *Food Res. Int.*, Vol. 62, pp. 326-343, 2014
- Ngan, H.Y.Y., Pang, G.K.H. and Yung, N.H.C., "Automated fabric defect detection – a review," *Image and Vision Computing*, Vol. 29, pp. 442–458, (2011).
- Crump, S.S., Comb, J.W., Priedeman Jr, W.R. and Zinniel, R.L., *Process of Support Removal For Fused Deposition Modeling*, US Patent No. 5503785 A, (1996).
- Pandey, P.M., Reddy, N. V. and Dhande, S.G., "Real time adaptive slicing for fused deposition modelling," *Int. J. Mach. Tool Manuf.*, Vol. 43, No.1, pp. 61-71, (2003).
- Agarwala, M.K., Jamalabad, V.R., Langrana, N.A., Safari, A., Whalen, P.J. and Danforth, S.C., "Structural quality of parts processed by fused deposition," *Rapid Prototyping*, Vol. 2, No.4, pp. 4-19, (1996).
- Boschetto, A., Bottini, L. and Veniali, F., "Finishing of Fused Deposition Modeling parts by CNC machining," *Robot. Comp.-Integra. Manuf.*, Vol. 41, pp. 92-101, (2016).
- Wu, S., Rangarajan, S., Dai, C., Langrana, N.A., Safari, A. and Danforth, S.C., "Warm Isostatic Pressing (WIP'ing) of GS44 Si3N3 FDC Parts for Defect Removal," *J. Mater. & Design*, Vol. 24, pp. 681-686, (2003).
- Bhandarkar, S.M., Luo, X., Daniels, R. and Tollner, E.W., "A novel feature-based tracking approach to the detection, localization, and 3-D reconstruction of internal defects in hardwood logs using computer tomography." *Pattern Anal. Appl.*, Vol. 9, No2-3, pp. 155-157, (2006).
- Fang, T., Jafari, M.A., Danforth, S.C. and Safari, A., "Signature analysis and defect detection in layered manufacturing of ceramic sensors and actuators," *Mach. Vision App.*, Vol. 15, No. 2, pp. 63-75, (2003).
- Luo, R.C., Tzou, J.H. and Chang, Y.C., "Desktop rapid prototyping system with supervisory control and monitoring through Internet," *IEEE/ASME Trans. Mechatron.*, Vol. 6, No. 4, pp. 399-409, (2001).
- Asselin, M., Toyserkani, E., Irvani-Tabrizipour, M. and Khajepour, A., "Development of Trinocular CCD-Based Optical Detector for Real-Time Monitoring of Laser Cladding," *Proc. IEEE Int. Conf. Mechatron. Automa.*, Vol. 3, pp. 1190-1196, (2005).
- Otsu, N., "A Threshold Selection Method from Gray-Level Histograms," *IEEE Trans. Sys., Man, Cybernet.*, Vol. 9, No. 1, pp. 62-66, (1979).
- Gauglitz, S., Höllerer, T. and M. Turk, "Evaluation of Interest Point Detectors and Feature Descriptors for Visual Tracking," *Int. J. Comp. Vision*, Vol. 94 No. 3, pp. 335-360, (2011).

基層製造熔融沉積成型至成影像監控之研究

蔡宏營 徐煒員 陳翼弘 曹哲之
國立清華大學 動力機械工程學系

摘要

本研究提出一種以積層製造的熔融塑料沉積成型技術為基礎，結合影像監控成型品質的布料技術，解決成型過程中產生的缺陷、品質難以掌控的問題。通過監控熔融沉積成型機台的噴嘴及被擠出熔融狀的材料之各項影像資訊，計算通過材料的實際高度、寬度等訊息，以準確控制噴嘴的給進，達成工件品質管控的目的。